AADE-05-NTCE-13

Wellbore Stability Model for Marine Sediments Containing Gas Hydrates

Richard Birchwood, Sheila Noeth, & Patrick Hooyman, Schlumberger Data and Consulting Services, Houston, Texas
William Winters, U. S. Geological Survey, Woods Hole, Massachusetts
Emrys Jones, ChevronTexaco, Houston, Texas

This paper was prepared for presentation at the AADE 2005 National Technical Conference and Exhibition, held at the Wyndam Greenspoint in Houston, Texas, April 5-7, 2005. This conference was sponsored by the Houston Chapter of the American Association of Drilling Engineers. The information presented in this paper does not reflect any position, claim or endorsement made or implied by the American Association of Drilling Engineers, their officers or members. Questions concerning the content of this paper should be directed to the individuals listed as author/s of this work.

Abstract

Predicting wellbore stability in shallow marine sediments can be a challenge if natural gas hydrates are present in the formation. Elevated wellbore temperatures during drilling can cause gas hydrates to dissociate, thereby significantly altering the mechanical properties of the sediments. This paper describes a prototype mechanical wellbore stability model (HYDRAPLASTIC ©), which was developed as part of the Gulf of Mexico Joint Industry Participation Agreement (JIP), sponsored by industry and the U.S. Department of Energy.

The model uses an elastoplastic Mohr-Coulomb formulation to predict shear failure. Assuming a plane-strain axisymmetric configuration, it calculates the mudweight window representing the zone of mechanical stability of wellbores in sediments containing gas hydrates. The code was benchmarked against a standard finite-element code (ABAQUS™) and includes a user-friendly GUI interface.

In order to account for the thermal sensitivity of hydrates, temperature modeling was conducted to determine the conditions for hydrate dissociation during drilling. This involved applying models to calculate the thermal properties of sediments containing gas hydrates. It was found that the circulation rate was a most critical factor in controlling hydrate stability. The overall influence of circulation rate and sediment salinity upon dissociation was demonstrated using a hypothetical field case.

Introduction

Gas hydrates are ice-like crystalline solids composed of a lattice of water molecules containing trapped gas molecules that stabilize the hydrate structure. Methane gas hydrates are the most common species of hydrate. However hydrates containing other hydrocarbons, such as propane and ethane, also exist. Additionally, non-hydrocarbon gases such as CO_2 and H_2S can be incorporated into the hydrate structure.

Gas hydrates are prevalent in permafrost regions and in the deeper marine environments of continental margins. In order for gas hydrates to form, methane and water at the appropriate pressure-temperature regime must be present. The stability of hydrates is also influenced by salinity and gas composition.

In nature, gas hydrates occur in the pore spaces of sediments, as veins as well as in thin layers, nodules and fracture fillings. In addition to residing in sediments, hydrates can form plugs in pipelines during gas production or drilling. Hydrate plugs can clog valves or chokes resulting in a loss of well control. The need to preempt this problem has been widely recognized by operators and the use of inhibitants in flowlines is a standard practice. However the geomechanical problems and hazards associated with drilling through sediments containing gas hydrates are less well recognized. This problem is especially relevant when drilling deepwater wells, where gas hydrates are stable at sea bottom pressures and temperatures and can form in shallow sediments. On the one hand, gas hydrates have the potential to enhance the mechanical stability of these sediments leading to more stable wellbores. On the other hand, temperature and pressure disturbances caused by the drilling process can lead to dissociation of gas hydrates, resulting in uncontrolled releases of gas into the wellbore, fires, and blowouts. The liberated gas can also gasify the drilling mud. Wellbore instability caused by sloughing of sedimentary sections containing dissociating gas hydrates could result in losing a hole or sidetracking[1]. Other problems are casing failure caused by gas leakage outside the casing and/or poor cement bonding in hydrate bearing sediments. An increase in formation pressure can occur in wells completed in gas hydrate bearing zones[2], because the production of hot hydrocarbons can lead to hydrate dissociation around a cased wellbore.

Interest in the resource potential of gas hydrates has provided a rationale for scrutinizing drilling practices in the shallow subsurface. The conventional oil industry drilling practice of jetting through the shallow subsurface results in poorly-gauged surface holes. Poor hole conditions can diminish the quality of logs in hydrate zones and compromise the integrity of completions leading to hazardous conditions such as gas seepage. If a more effective drilling strategy is to be realized,

accurate models of borehole stability in shallow marine sediments are required. Borehole stability models that fail to account for the mechanical effects of gas hydrates run the risk of being unnecessarily conservative and are therefore likely to lead to inefficient drilling practices. Elastic-brittle models are prone to similar shortcomings when they are applied to the soft plastic sediments of the shallow subsurface. Finally, because of the pronounced temperature sensitivity of gas hydrates, the impact of temperature on hole stability must be considered.

Taking these facts into consideration, an elastoplastic wellbore stability model was developed within the framework of the Gulf of Mexico Gas Hydrates Joint Industry Participation Agreement (JIP), in which several petroleum producers, service companies, universities and government institutions are participating. The multiyear industry/DOE sponsored program is managed by ChevronTexaco. Its primary objective is the characterization of natural gas hydrates in the deep water Gulf of Mexico region. To help further this objective, a wellbore stability model, known as HYDRAPLASTIC©, was designed to simulate the mechanical failure of sediments containing gas hydrates. Additional modeling was conducted using a temperature simulator to determine the conditions under which hydrates might dissociate as a result of drilling-induced temperature disturbances.

Benchmarking the Wellbore Stability Model

The development of the wellbore stability code was initiated after an extensive review of existing software revealed the need for a computer code that could handle wellbore stability analysis in hydrate-bearing formations[3]. The purpose of the code is to calculate the mudweight window representing the zone of mechanical stability of wellbores drilled in formations typical of those in which gas hydrates could be found. Such formations would be expected to consist of weak or unconsolidated sediments containing varying amounts gas hydrates. The code uses a Mohr-Coulomb plasticity model to predict shear failure. A plane-strain axisymmetric geometry is assumed, consistent with vertical wells drilled in horizontally isotropic stress fields. Such stress fields would be expected to occur in shallow relaxed-basin sediments such as those found in the Gulf of Mexico.

The appropriateness of the Mohr-Coulomb plasticity model was determined by comparing the predictions of the model with data obtained from triaxial tests conducted on samples containing THF hydrate (Birchwood et al*., in prep*). The tests were performed by the Georgia Institute of Technology under the sponsorship of the JIP[4]. Figure 1 illustrates the analysis of data derived from experiments on sand with a 50% hydrate saturation subject to confining pressures of 30, 500, and 1000 kPa. For this case, a satisfactory fit to a cohesion hardening Mohr-Coulomb model was obtained (Figure 1(a)) resulting in a good match between the modeled and experimental stress-strain curves (Figure 1(b)).

The wellbore stability code solves a fast semi-analytical formulation for the plastic strains around the borehole wall. The solution was developed by *Bradford and Cook*[5] and was designed as an alternative to computationally intensive numerical schemes that are impractical for producing borehole logs. The borehole is assumed to fail when the equivalent plastic strain exceeds a critical value. In order to simplify the formulation, *Bradford and Cook* made two approximations that could potentially produce departures from an exact plane-strain solution. First, in order to integrate the plastic strain increments analytically, a proportional loading path was assumed. This assumption is only strictly true for a model employing the associated flow rule. The integration becomes inexact as the difference between the dilation and friction angles increases.

Second, the plastic potential was chosen to be independent of the vertical effective stress, σ'_{zz} thereby forcing the corresponding plastic strain, ε_{zz}^{p} to zero. In a plane strain solution only the total strain, ε_{zz}, (equal to the sum of the elastic and plastic strains), is set to zero.

In spite of these limitations, the results of benchmarking indicate that the semi-analytical formulation produces satisfactory estimates of stress and strain around the borehole wall. The formulation was benchmarked against ABAQUS™. Two cases are shown in Figures 2 and 3. In Figure 2, the dilation and friction angles were both set to 16^{o} whereas in Figure 3, the dilation angle was reduced to 3^{o}. In Figure 2(a) the stresses computed by the semi-analytical formulation coincide with the stresses computed by ABAQUS™ almost exactly. However because of the second simplification discussed in the preceding paragraph, slight differences between the two sets of strains can be seen (Figure 2(b)).

In Figure 3(a) the stresses are again in excellent agreement, however the semi-analytical formulation has a tendency to underestimate the plastic strains as the proportional loading assumption is violated (Figure 3(b)). This error however is generally small.

Temperature Modeling

A temperature simulator was used to investigate the conditions under which hydrates could dissociate during drilling. It was assumed that there was a risk of dissociation if the temperature in the formation exceeded the phase-change temperature. This risk criterion is conservative since it ignores the kinetics of dissociation. However simulating the kinetics of dissociation would involve evaluating the energy exchange between the

drilling fluid, the hydrate, and any gas that is produced. Such considerations lay beyond the scope of the project.

As a prerequisite for the simulations, the thermal properties of hydrate bearing sediments were estimated. The estimation methods are described in the following subsections.

Specific Heat Capacity

The bulk specific heat capacity of the sediment was calculated using the following weighted average:

$$c_p = \frac{1}{m}\sum_i \rho_i c_{pi} \mathrm{V}_i$$

where the densities and specific heat capacities of the constituents are given in Tables 1 and 2 respectively.

Thermal Conductivity

The bulk thermal conductivity of the sediment was determined using a random spheroidal grain inclusion model developed for soils by de Vries[6]. Thermal conductivities were computed for sandy and clayey sediments containing various amounts of water, methane gas, methane hydrate, and ice. Hydrates were modeled as separate grains within the matrix or constrained to coat the grains of the host rock by applying the de Vries formula twice. In the first application of the formula, the average thermal conductivity of the host grain embedded in a methane hydrate background was computed. This gave the average thermal conductivity of a grain coated by methane hydrate. For the second application of the formula, the average thermal conductivity of the entire mixture was estimated. Table 3 shows the thermal conductivities that were assumed for the constituents.

Field Example

A hypothetical field example based loosely upon data acquired from Blake Ridge and the Gulf of Mexico formed the basis for a temperature modeling study. The objective of the study was to determine the drilling practices most likely to lead to hydrate dissociation. Figure 4 shows the setting of the study known as Site A. The water depth was 4300 ft. The ambient temperature and methane hydrate phase boundary are superimposed over the diagram. The latter was computed using methods devised by Kamath[7] and is based upon an assumed uniform salinity of 3.5% NaCl concentration by weight. The intersection of the geothermal gradient and the hydrate phase boundary defines the base of the hydrate stability zone some 1600 ft below the mudline.

In order to compute the thermal properties of the sandy sediments, a mineral composition consisting of 80% quartz and 20% clay was assumed. For the clay sediments, the assumed composition was 60% clay, 5% quartz, and 35% calcite. This latter composition was the same as that used by Helgerud (2001)[8] to estimate the hydrate saturation in Blake Ridge, ODP Leg 164, Site 995. The porosity was estimated from a density log at Site 995 and then fitted to an exponential curve (Figure 5). The same exponential trend was then assumed at Site A.

The resulting thermal properties are shown in Figures 6 and 7. The compositions shown are based mainly upon the range of compositions hypothesized for Blake Ridge[8]. It may be observed that (a) the specific heat capacity of the clay sediment is greater than that of the sand, whereas the opposite holds true for the thermal conductivity; (b) sediments that are 100% saturated with water have the highest specific heat capacity whereas those containing ice have the lowest; (c) ice produces sediments with the highest thermal conductivity while methane gas is the best thermal insulator; and (d) when hydrate coats the grains, it has a greater insulating effect than when it resides in the pore space.

In a rather surprising twist, temperature simulations showed that for the drilling program at Site A, the temperature at the borehole wall during drilling was not highly sensitive to the values of K and c_p when these were varied within a reasonable range (Figure 8). However to establish what constituted a reasonable range, it was necessary to first compute these properties in detail. Figure 8 also shows that increasing either K or c_p has a tendency to increase the borehole wall temperature, with K having a slightly larger effect.

A set of conditions most conducive to hydrate dissociation was chosen so that conservative estimates of the risk of dissociation during drilling could be made. For the formation it was assumed that K and c_p were uniformly equal to 2 W/m^2.K and 2500 J/kg.K respectively. The drilling fluid was assumed to be seawater conveyed through a riserless 5-1/2 inch drillpipe to the sea bottom. The temperature of the drilling fluid entering the drillpipe was set to 90^{o}F (32.3^{o}C). A geothermal gradient of 25^{o}C/km was assumed and the temperatures induced by drilling a vertical 8-1/2 inch diameter hole to a depth of 1700 ft below the mudline were calculated. The drilling plan consisted of continuous drilling at a constant ROP to TD, followed by 2 hours of circulation.

Figure 9(a) shows the results of drilling with an ROP of 100 ft/hr while maintaining a constant circulation rate of 350 gal/min. For the standard seawater salinity of 3.5 % NaCl, the temperature at the borehole wall is much less than the hydrate dissociation temperature, so there is little risk of dissociation. However for a much higher salinity of 15% NaCl, the temperature at the wellbore wall coincides with the hydrate phase stability temperature. Hydrates existing in the stable zone extending some 500 ft below the mudline would be at risk of dissociating. A salinity of 15% is unusually high but not out of the question – overall salinities in excess

of 20% have been observed in the Mississippi Fan, Gulf of Mexico, near salt diapers outcropped at the seafloor[9].

Figure 9(b) shows that increasing the circulation rate to 500 gal/min exacerbates dissociation for two reasons. First, as the circulation rate increases, the residence time of the fluid in the ocean section of the drillpipe decreases, resulting in a reduction of heat dissipated to the ocean. Consequently the drilling fluid is hotter when it arrives at the sea bottom. This effect can be seen quite clearly by comparing tubing temperatures at the mudline in Figures 9(a) and (b).

Second, larger flow rates lead to increased viscous dissipation within the drillpipe particularly around the convergent zone at the bit nozzle. This dissipation is responsible for the significant difference in the temperature of the drilling fluid entering and leaving the borehole which can be seen by comparing the tubing and borehole wall temperatures at the mudline (Figure 9(b)). From Figure 9(c) it can be concluded that the probability of dissociation can be reduced by circulating at a lower rate of 250 gal/min. Figure 9(d) shows that reducing the ROP to 50 ft/hr does little to affect the risk of hydrate dissociation (c.f. Figure 9(a)).

Conclusions

A semi-analytical Mohr-Coloumb elastoplastic code called HYDRAPLASTIC © has been developed for analyzing the stability of wellbores drilled in gas hydrates. Benchmarking of the code against the ABAQUS™ finite-element simulator shows that the semi-analytical formulation predicts borehole stresses associated with the plane strain condition almost exactly and that errors in the plastic strains occurring as a result of the approximations used to simplify the mathematics are small.

Temperature simulations were performed to determine the conditions under which hydrate dissociation could occur while drilling with seawater in a hypothetical field. A sensitivity study was carried out to ascertain the typical ranges of thermal properties that could be expected in the field. It was observed that the temperature at the wellbore wall was not particularly sensitive to the formation thermal properties when these were varied within an expected range.

The simulations showed that for normal pore water salinities, the risk of dissociation due to drilling induced temperature disturbances was small for moderate circulation rates. However at high salinities the risk of dissociation greatly increased. Reduction of the circulation rate was shown to be an effective strategy for reducing the risk of dissociation.

Acknowledgments

We wish to acknowledge the valuable assistance of Colin Sayers, Francis Elisabeth, Dick Plumb, Robert Marsden, Ian Bradford, Yan GongRui, and Vladimir Tertychnyi of Schlumberger; J. Carlos Santamarina and Carolyn Ruppel of the Georgia Institute of Technology; and Ben Bloys, Aaron Conte, and Sivakumar Subramanian of ChevronTexaco.

Nomenclature

a = *uniaxial yield strength*
b = *coefficient multiplying power law term in strain hardening equation*
c_p = *specific heat capacity in (J/kg.K)*
E = *Young's modulus*
K = *thermal conductivity (W/m.K)*
m = *mass*
n = *exponent in power law strain hardening equation*
p = *ambient pressure*
p_p = *pore pressure*
p_w = *wellbore pressure*
r = *distance from center of borehole*
r_o = *radius of borehole*
ROP = *drilling rate of penetration*
T = *temperature (^oC)*
TD = *total depth*
v = *specific volume*
ϕ = *friction angle*
ν = *Poisson's ratio*
ρ = *density*
σ_h = *horizontal stress*
σ_v = *vertical stress*
ψ = *dilation angle*

References

1. Collett, T.S. and Dallimore, S.R.: "Detailed analysis of gas hydrate induced drilling and production hazards," *4th International Conference on Gas Hydrates (ICGH-4), Yokohama, May* (2002).

2. Franklin, L.J.: "Hydrates in Artic Islands," In: A.L. Browser: *Proceedings of a Workshop on Clathrates (gas hydrates) in the National Petroleum reserve in Alaska*. *USGS Open-File Report 81-1259,* 18-21, (1981).

3. Noeth, S., Plumb, D., Hooyman, P., and Ivanova, V.: "Proposal to develop a wellbore stability model for formations containing natural gas hydrates," *Status Report for Phase I (Task 5.1)*, prepared by Schlumberger Data and Consulting Services for ChevronTexaco Exploration and Production Technology Company Gulf of Mexico Gas Hydrates Joint Industry Participation Project (JIP), Houston, Texas. (2003).

4. Santamarina, J.C., Francisca, F., Yun, T.-S., Lee, J.-Y., Martin, A.I., and Ruppel, C.: "Mechanical, thermal, and electrical properties of hydrate-bearing sediments," *AAPG Hedburg Research Conference, Vancouver, Sep.*

12-16, (2004).

5. Bradford, I.D.R. and Cook, J.M.: "A semi-analytical elastoplastic model for wellbore stability with applications to sanding," *Proceedings of the SPE/ISRM Rock Mechanics in Petroleum Engineering Conference*, Delft, The Netherlands, Aug. 29-31, 1994, 347-354. (SPE Paper No. 28070)

6. de Vries, D.A.: "Thermal Properties of soils," In: R. van Wijk (ed.): *Physics of Plant Environment*. North Holland, Amsterdam, (1963), 210-235.

7. Kamath, V.A., *Personal communication*.

8. Helgerud, M. "Wave speeds in gas hydrate and sediments containing gas hydrate: a laboratory and modeling study," *Ph.D. Dissertation*, Stanford University, (2001)

9. Ishizuka, T., Kawahat, H., and Aoki, S.: "Interstitial water geochemistry and clay mineralogy of the Mississippi Fan and Orca and Pigmy Basins, Deep Sea Drilling Project Leg 96," *Initial Reports of the Deep Sea Drilling Project*, v. XCVI*,* 711-727.

10. Mavko, G., Mukerji, T. and Dvorkin, J.: "*The Rock Physics Handbook: Tools for Seismic Analysis in Porous Media*," Cambridge University Press, 329 pp. (1998)

11. Batzle, M. and Wang, Z.: "Seismic properties of pore fluids," *Geophys*. v. 57, (1992). 1396-1408.

12. Dvorkin, J., Helgerud, M. B., Waite, W.F., Kirby, S.H. and Nur, A.: "Introduction to Physical Properties and Elasticity Models," In: M.D. MAX (ed.): *Natural Gas Hydrate in Oceanic and Permafrost Environments*. Kluver Academic Publishers. (2000). 245-260.

13. Butler, R.M.: "*Thermal Recovery of Oil and Bitumen*," Prentice-Hall Inc., 514 pp. (1991).

14. Schön, J.H.: "*Physical Properties of Rocks: Fundamentals and Principles of Petrophysics,"* Pergamon, 583 pp. (1995).

15. Reid, R. C., Prausnitz, J. M. and Poling, B. E.: "*The Properties of Gases and Liquids*," McGraw-Hill, 735 pp. (1987).

16. Handa, Y.P.: "Compositions, enthalpies of dissociation, and heat capacities in the range 85 to 270 K for clathrate hydrates of methane, ethane, and propane, and enthalpy of dissociation of isobutene hydrate, as determined by a heat-flow calorimeter," *Journal of Chemical Thermodynamics, vol. 18, (*1986), 915-921.

17. Cook, J.G. and Leaist, D.G.:"An exploratory study of the thermal conductivity of methane hydrate," *Geophys. Res. Lett.* V. 10, (1983). 397-399.

Table 1: Densities of constituents

Substance	ρ	Reference
Seawater (35 ppm salinity)	1025 kg/m^3	U.S. DOT Chemical Hazards Response Information System*
Ice	919 kg/m^3	U.S. DOT Chemical Hazards Response Information System*
Clay	2580 kg/m^3	Mavko et al. 1998)[10]
Quartz	2650 kg/m^3	
Calcite	2710 kg/m^3	Mavko et al. (1998)[10]
Methane Gas	Algorithm due to Batzle and Wang†	Batzle and Wang (1992)[11]
Methane Hydrate	910 kg/m^3	Dvorkin et al. (2000)[12]

Table 2: Specific Heat Capacities of Constituents.

Substance	c_p	Reference
Seawater (35 ppm salinity)	3900 J/kg.K	U.S. DOT Chemical Hazards Response Information System*
Ice	2100 J/kg.K	U.S. DOT Chemical Hazards Response Information System*
Clay	$726+1.43T-1.959\times10^{-3}T^2+1.731\times10^{-6}T^3$ J/kg.K	Adapted from Butler (1991)[13]
Quartz	$715+1.707T-1.908\times10^{-3}T^2$ J/kg.K	Butler (1991) [13]
Calcite	793 J/kg.K	Schon (1996)[14]
Methane Gas	Lee-Kesler Method‡	Reid (1987)[15]
Methane Hydrate	$2102.9+7.08146T+0.0123578T^2 +5.09032\times10^{-5}T^3$ J/kg.K	Adapted from Handa (1986)[16]

Table 3: Thermal Conductivities of Constituents

Substance	K	Reference
Seawater (35 ppm salinity)	0.577 W/m.K	U.S. DOT Chemical Hazards Response Information System*
Ice	2.24 W/m.K	U.S. DOT Chemical Hazards Response Information System*
Clay	2.2 W/m.K	Adapted from Butler (1991) [13]
Quartz	7.7 W/m.K	Butler (1991) [13]
Calcite	3.57 W/m.K	Butler (1991) [13]
Methane Gas	Method due to Chung (for high pressures)§	Reid (1987)[15]
Methane Hydrate	0.45 W/m.K	Cook & Leaist (1983)[17]

* http://www.chrismanual.com/

† As a reference, $\rho = 135$ kg/m^3 at $T = 10^oC$, $p = 150$ atm

‡ As a reference, $c_p = 3620$ J/kg.K at $T = 10^oC$, $p = 150$ atm

§ As a reference, $K = 0.052$ W/m.K at $T = 10^oC$, $p = 150$ atm

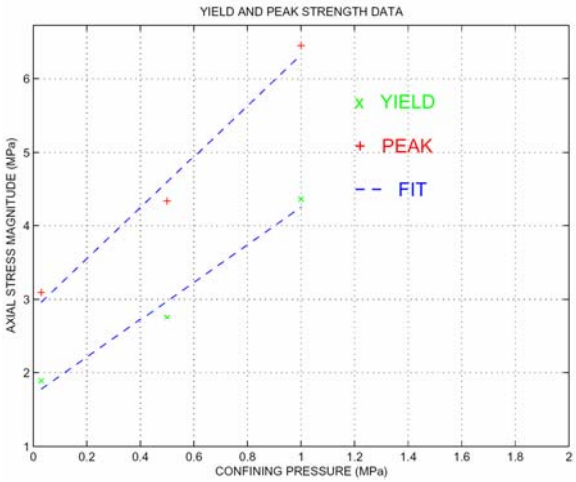

Fig. 1(a) - Modeling triaxial test data for sand with a 50% hydrate saturation. Linear fits to yield and peak strength data shown.

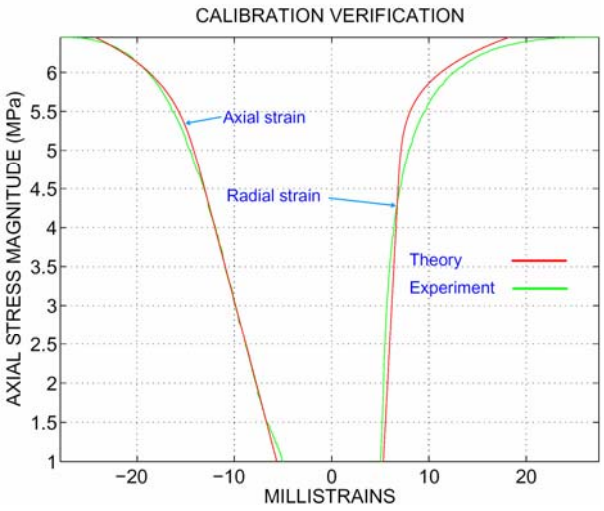

Fig. 1(b)- Comparison between theoretical and experimental stress-strain curves (confining pressure = 1000 kPa).

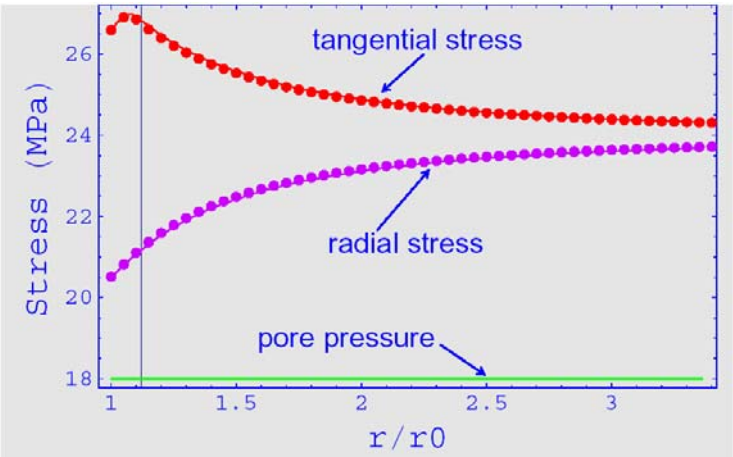

Fig. 2(a) - Comparison of borehole stresses computed by semi-analytical formulation (solid lines) with those computed by ABAQUS™ (dots). p_w = 20.5 MPa, σ_h = 24 MPa, p_p = 18 MPa, E = 150 MPa, ν = 0.38, a = 3.2 MPa, b = 2.8 MPa, n =0.2, $\phi = \psi = 16^O$.

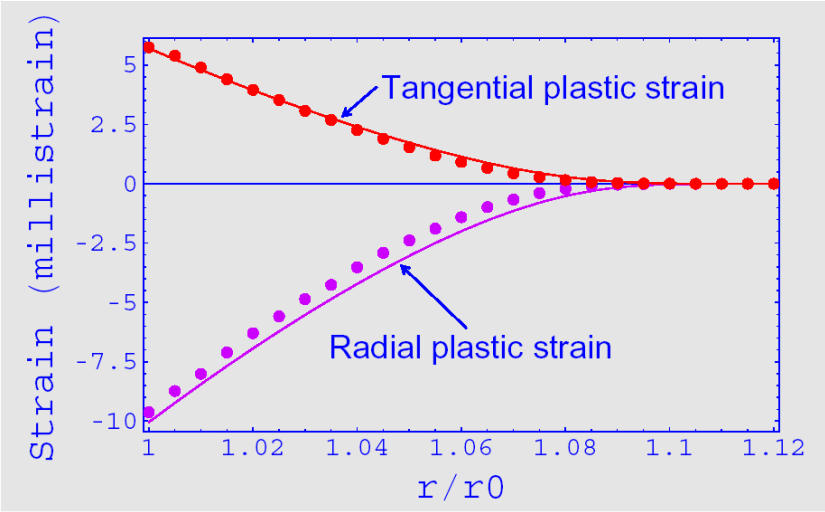

Fig. 2(b)- Comparison of borehole plastic strains computed by semi-analytical formulation (solid lines) with those computed by ABAQUS™ (dots). p_w = 20.5 MPa, σ_h = 24 MPa, p_p = 18 MPa, E = 150 MPa, ν = 0.38, a = 3.2 MPa, b = 2.8 MPa, n =0.2, $\phi = \psi = 16^O$.

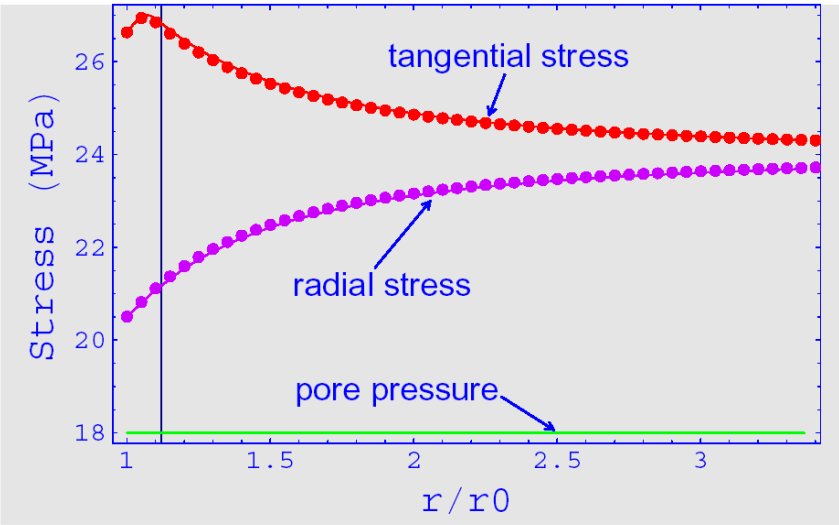

Fig. 3(a)- Comparison of borehole stresses computed by semi-analytical formulation (solid lines) with those computed by ABAQUS™ (dots). p_w = 20.5 MPa, σ_h = 24 MPa, p_p = 18 MPa, E = 150 MPa, ν = 0.38, a = 3.2 MPa, b = 2.8 MPa, n =0.2, ϕ=16^0 ψ= 3^0.

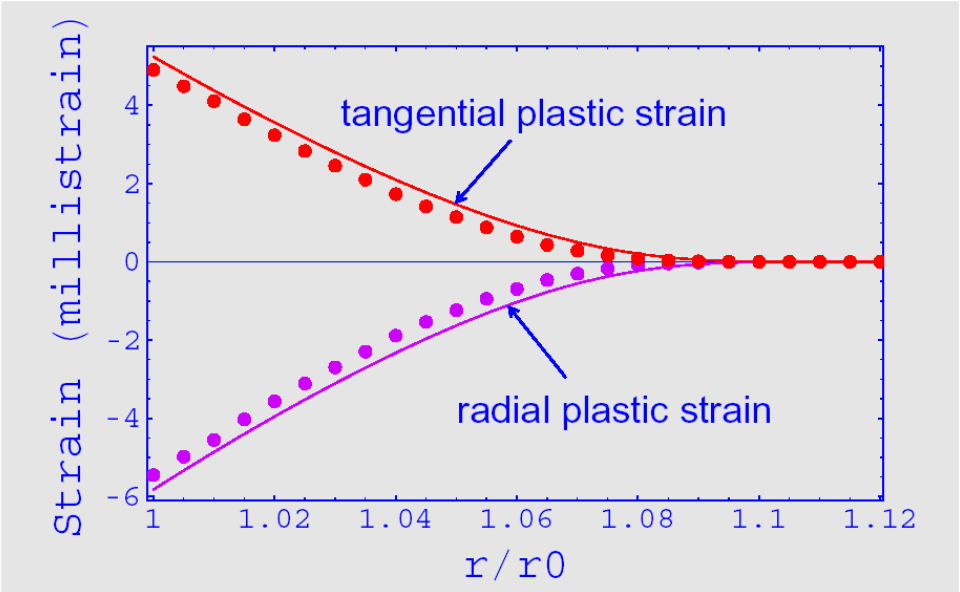

Fig. 3(b)- Comparison of borehole plastic strains computed by semi-analytical formulation (solid lines) with those computed by ABAQUS™ (dots). p_w = 20.5 MPa, σ_h = 24 MPa, p_p = 18 MPa, E = 150 MPa, ν = 0.38, a = 3.2 MPa, b = 2.8 MPa, n =0.2, ϕ=16^0 ψ= 3^0.

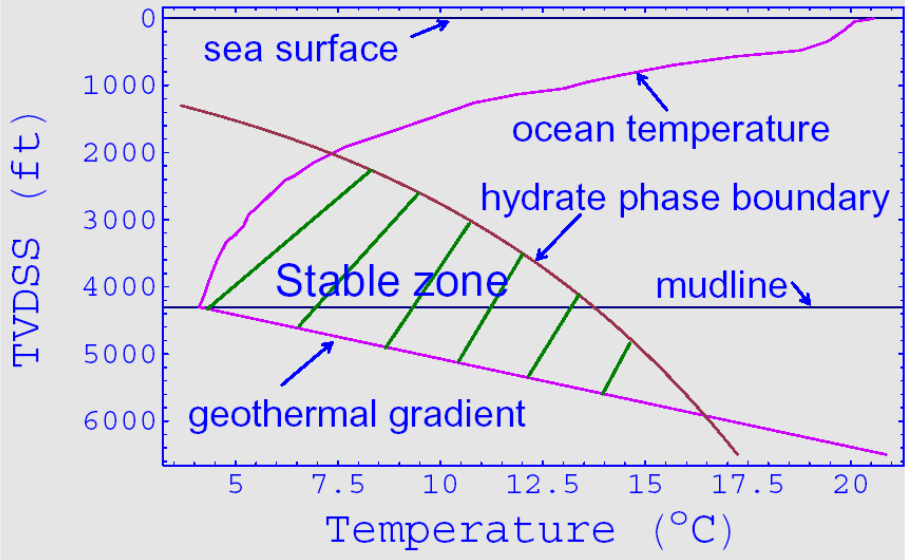

Figure 4 – Setting of Site A

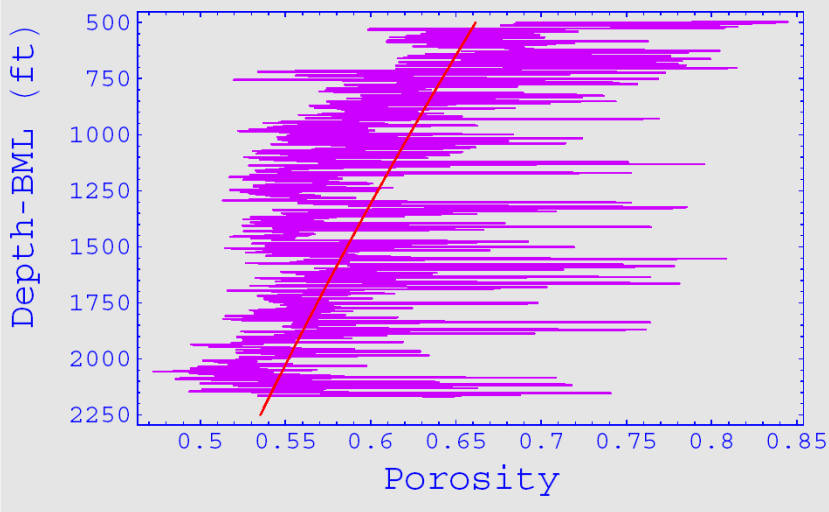

Figure 5– Porosity depth-profile adapted from Blake Ridge (purple) and exponential curve fit (red)

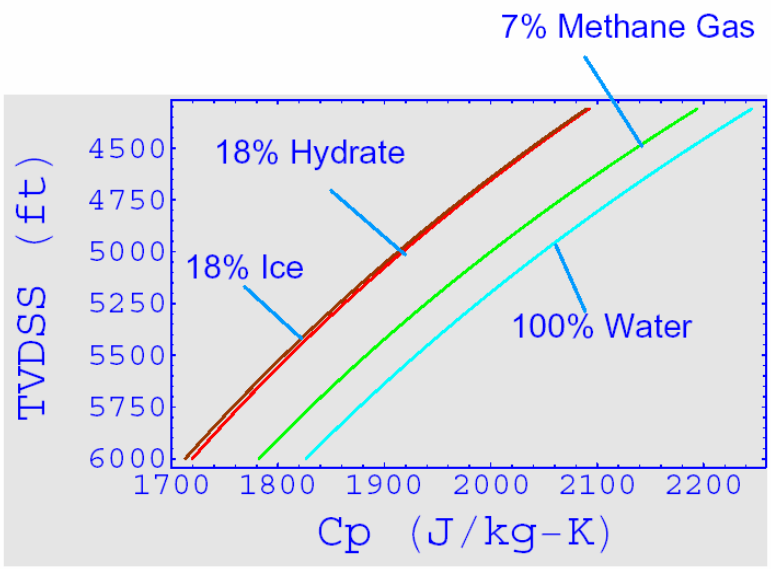

Figure 6(a) – Depth dependence of specific heat capacity for sandy sediment containing water and various other constituents.

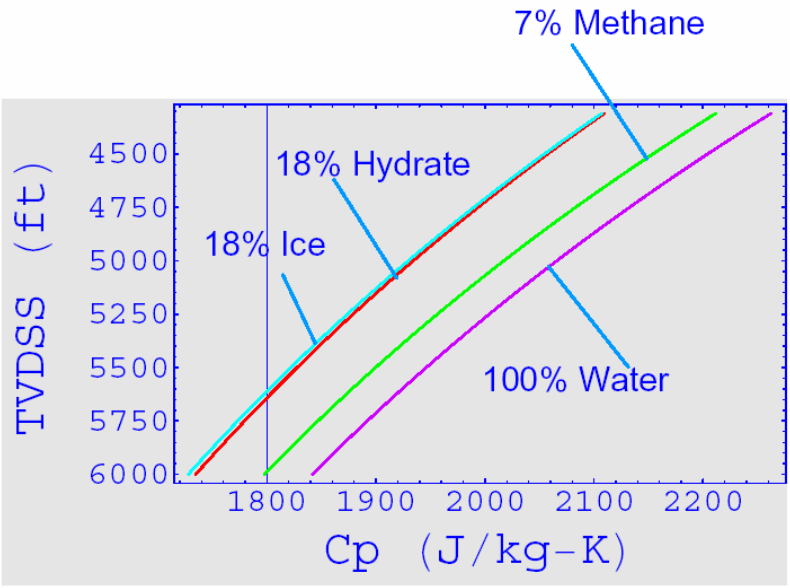

Figure 6(b) – Depth dependence of specific heat capacity for clayey sediment containing water and various other constituents.

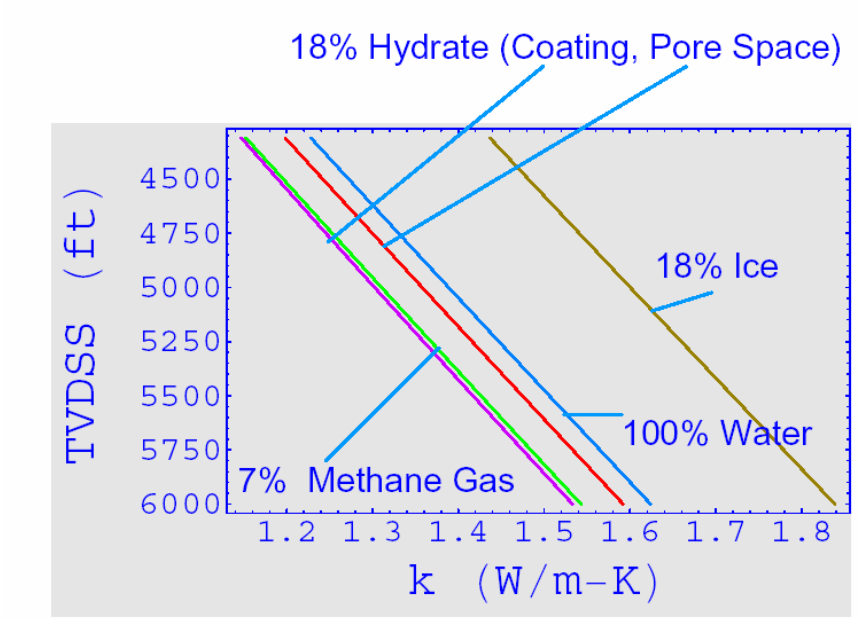

Figure 7(a) – Depth dependence of thermal conductivity for sandy sediment containing water and various other constituents.

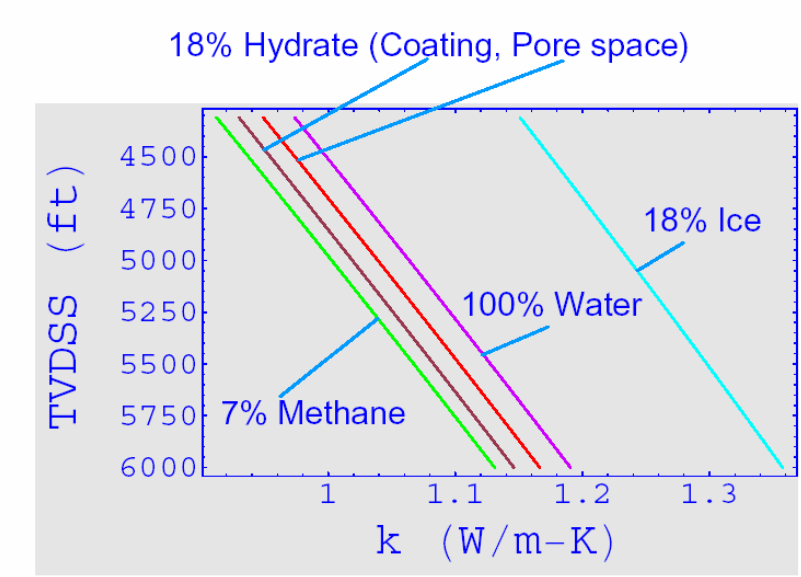

Figure 7(b) – Depth dependence of thermal conductivity for clayey sediment containing water and various other constituents.

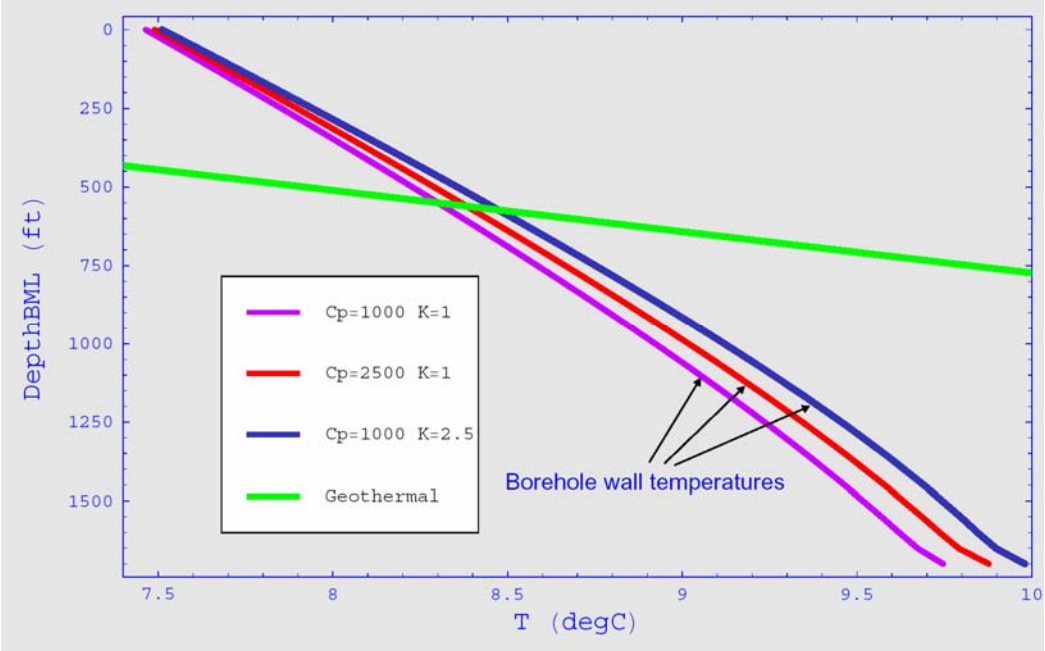

Figure 8 – Temperature at the borehole wall versus depth below mudline for various formation thermal properties. Temperature profiles plotted after 17 hrs of continuous drilling at ROP of 100 ft/hr. A geothermal gradient of 25°C/km is also shown. The circulation rate was 350 gal/min.

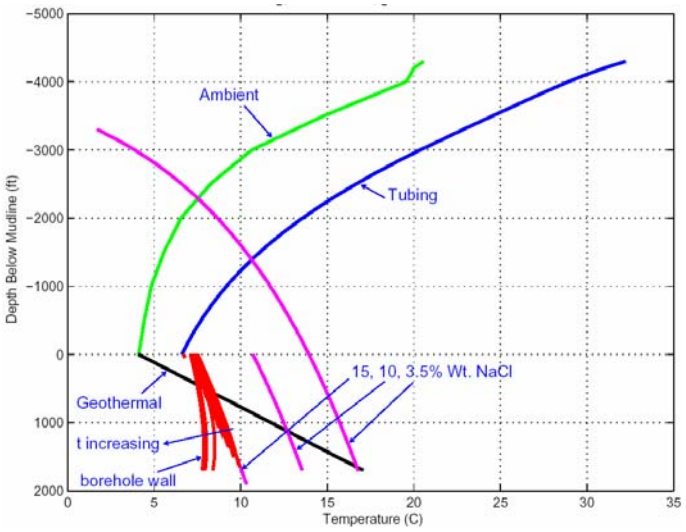

Figure 9(a) – Temperatures associated with drilling at ROP of 100 ft/hr for 17 hours and then circulating for 2 hours. Circulation rate of 350 gal/min maintained during both phases. Temperatures in ocean (green), tubing (blue), virgin sediment (black) and at borehole wall (red) shown along with methane hydrate phase stability boundaries (magenta) computed at various sodium chloride concentrations. Wall temperature profiles, which are shown at different times, curve sharply to the left during circulation.

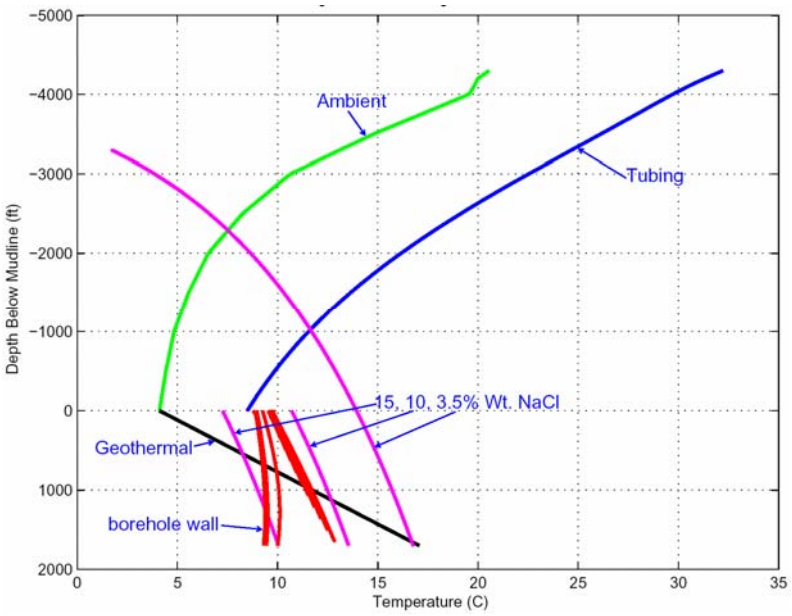

Figure 9(b) – Temperatures associated with drilling at ROP of 100 ft/hr for 17 hours and then circulating for 2 hours. Circulation rate of 500 gal/min maintained during both phases. Temperatures in ocean (green), tubing (blue), virgin sediment (black) and at borehole wall (red) shown along with methane hydrate phase stability boundaries (magenta) computed at various sodium chloride concentrations. Wall temperature profiles, which are shown at different times, curve sharply to the left during circulation.

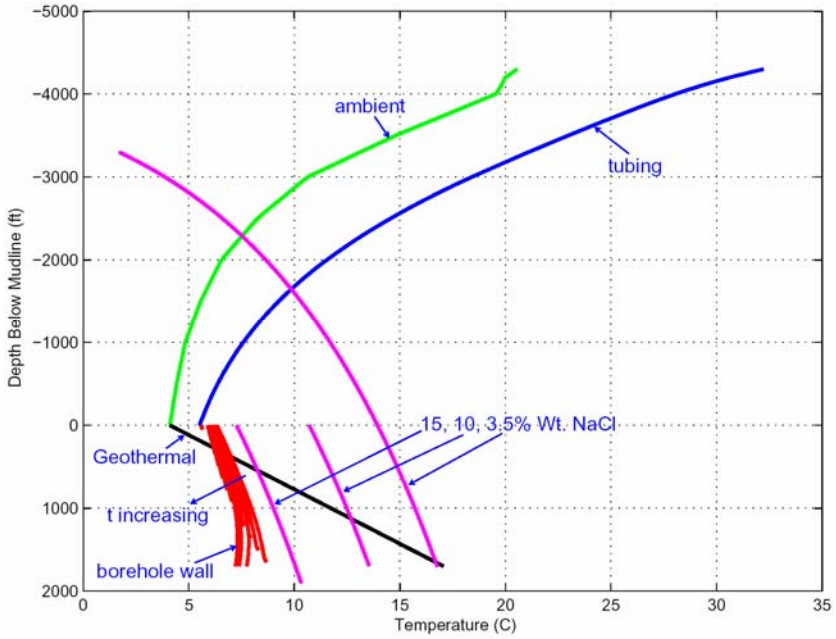

Figure 9(c) – Temperatures associated with drilling at ROP of 100 ft/hr for 17 hours and then circulating for 2 hours. Circulation rate of 250 gal/min maintained during both phases. Temperatures in ocean (green), tubing (blue), virgin sediment (black) and at borehole wall (red) shown along with methane hydrate phase stability boundaries (magenta) computed at various sodium chloride concentrations. Wall temperature profiles, which are shown at different times, curve sharply to the left during circulation.

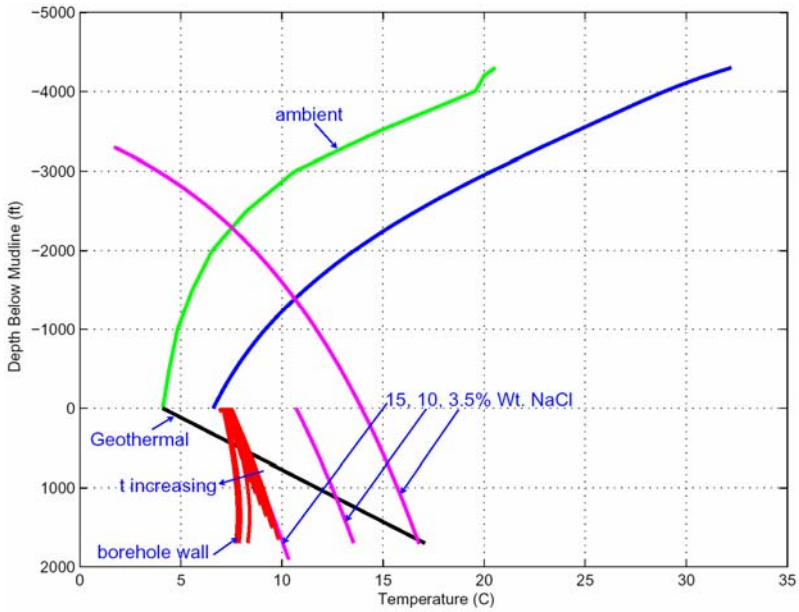

Figure 9(d) – Temperatures associated with drilling at ROP of 50 ft/hr for 34 hours and then circulating for 2 hours. Circulation rate of 350 gal/min maintained during both phases. Temperatures in ocean (green), tubing (blue), virgin sediment (black) and at borehole wall (red) shown along with methane hydrate phase stability boundaries (magenta) computed at various sodium chloride concentrations. Wall temperature profiles, which are shown at different times, curve sharply to the left during circulation.